Santoso, Imam; Taskinen, Pekka; Jokilaakso, Ari; Paek, Min; Lindberg, Daniel

Phase equilibria and liquid phase behavior of the K2O-CaO-SiO2 system for entrained flow biomass gasification

Published in:
Fuel

DOI:
10.1016/j.fuel.2019.116894

Published: 01/04/2020

Document Version
Publisher's PDF, also known as Version of record

Please cite the original version:
Santoso, I., Taskinen, P., Jokilaakso, A., Paek, M., & Lindberg, D. (2020). Phase equilibria and liquid phase behavior of the K2O-CaO-SiO2 system for entrained flow biomass gasification. *Fuel*, *265*(7), Article 116894. https://doi.org/10.1016/j.fuel.2019.116894

Fuel 265 (2020) 116894

Contents lists available at ScienceDirect

Fuel

journal homepage: www.elsevier.com/locate/fuel

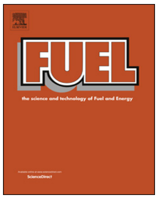

Full Length Article

Phase equilibria and liquid phase behavior of the K_2O-CaO-SiO_2 system for entrained flow biomass gasification

Imam Santoso[a,b,*], Pekka Taskinen[a], Ari Jokilaakso[a], Min-Kyu Paek[a], Daniel Lindberg[a,*]

[a] School of Chemical Engineering, Aalto University, Espoo, Finland
[b] Department of Metallurgical Engineering, Institut Teknologi Bandung, Bandung, Indonesia

ARTICLE INFO

Keywords:
Viscosity
EPMA
Biomass
Phase diagram
Slag

ABSTRACT

Experimental data of solid-liquid phase equilibria in the K_2O-CaO-SiO_2 systems vital for many technologies and industrial applications are very limited and even not available at some primary phase fields. In the present study, by using Equilibration-Quenching-Phase compositional analysis (EPMA/EDS) method, liquidus compositions in equilibrium with pure solid SiO_2, CaO·SiO_2, 3CaO·2SiO_2, 2CaO·SiO_2, K_2O·6CaO·4SiO_2 and K_2O·2CaO·2SiO_2 compounds and 2CaO·SiO_2 solid solution were measured. By knowing the evaporation behavior of K_2O during the equilibration process, specific initial mixtures could be selected to obtain liquidus data for targeted final equilibrium assemblages. EPMA and EDS analysis results were compared. The experimental data obtained in the present study were discussed and compared with the results from previous experimental investigations and the assessed ternary phase diagrams. Some novel experimental data of the liquid at single and double solid phase saturations were obtained in the present study and they can be used to correct and support the predictions and thermodynamic assessments of the K_2O-CaO-SiO_2 system. Present investigation reports liquidus projections and detailed phase relations among the phases in isothermal sections at 1000, 1100, 1200, 1300 and 1400 °C. Viscosity calculations of the liquid at different compositions between 1000 and 1400 °C also have been made. A combination of phase equilibria study and the viscosity predictions in the present investigation provides suitable temperature and ash composition regions for optimal flow properties of the slag in entrained flow biomass combustion or gasification processes.

1. Introduction

The most well-known and widely used phase equilibria of K_2O-CaO-SiO_2 system is the diagram obtained by Morey et al. [1,2] in 1930s as tabulated in Phase Diagram for Ceramists [3] and Slag Atlas compilations [4]. These fundamental data of K_2O-CaO-SiO_2 system are widely used in the glass and ceramics industries. For advanced ceramic applications, the K_2O-CaO-SiO_2 system is an important glass to make biocompatible ceramic material for biomedical applications [5]. For pyrometallurgical processes, the system is vital during smelting because the potassium fluxing can reduce the melting point of slag, decrease the viscosity [6] and to control the impurity distributions to the molten metal [7]. In energy and biomass industry, the K, Ca and Si are typically the most common ash-forming elements in most woody biomass fuels [8]. In biomass gasification, the K_2O-CaO-SiO_2 system can form a flowing slag on the walls of entrained flow gasifiers during production of the syngas [9]. Failure to understand the behavior of the system can cause serious catastrophic blockage of the reactor [10,11]. In fluidized bed combustion of biomass, the formation of K-Ca-silicates layers on the sand particles can lead to agglomeration of the bed [12]. The system is also important component in the potassium silicate fertilizer because the slow rate release of potassium ion to the soil can minimize the carry-over of the chemicals from the farming field to the surrounding environment [13]. Therefore, the data on this system is vital for process optimizations in many industries to make their practices more beneficial and sustainable to meet the strict environment regulations nowadays.

Unfortunately, the experimental studies of this system are not only limited but also there are some omissions of the liquidus data in several primary fields and even clear disagreement among the authors is observed. For example, the K_2O·CaO·SiO_2 primary phase field in the ternary diagram was reported to be stable by Morey et al. [1,2]. This compound also was observed by Ohsato et al. [14], Risnes [15] and Taylor [16]. However, K_2O·CaO·SiO_2 does not exist in the stable ternary system according to Arroyabe et al. [17] and Bankole et al. [18]. Thus, Chen et al. [19] reported the primary phase of K_2O·2CaO·2SiO_2 instead

---

* Corresponding authors.
E-mail addresses: imam.santoso@metallurgy.itb.ac.id (I. Santoso), daniel.k.lindberg@aalto.fi (D. Lindberg).

https://doi.org/10.1016/j.fuel.2019.116894
Received 1 September 2019; Received in revised form 25 October 2019; Accepted 14 December 2019

of $K_2O{\cdot}CaO{\cdot}SiO_2$. Moreover, some important parts of the ternary diagram are only extrapolated and predicted. For example, the $3CaO{\cdot}2SiO_2$ primary phase field in the ternary system was predicted by Morey et al. [1], extending from the binary CaO-SiO_2 section towards ternary field and it disappeared below 1400 °C. Thus, below 1400 °C the primary phase field of $2CaO{\cdot}SiO_2$ was drawn to be connected with the field of $CaO{\cdot}SiO_2$ and not $3CaO{\cdot}2SiO_2$ which was also assumed by Chen et al. [19]. However, a recent calculation by MTDATA [20], using the Mtox vers 8.2 database [21], indicated that below 1400 °C, $3CaO{\cdot}2SiO_2$ primary phase field is still there. This also agrees with FactSage 7.3 prediction, using FTOxide database [22]. Therefore, novel experimental data are required to support these predictions. Morey at al. [1] and Chen et al. [19] extrapolated the intersection between the SiO_2 and $CaO{\cdot}SiO_2$ primary phase fields and also between the $CaO{\cdot}SiO_2$ and $3CaO{\cdot}SiO_2$ primary phase fields. Thus, liquidus data at these double solid crystal saturations with the liquid phase are needed to indicate where exactly these primary phase fields meet and form the three phase equilibria.

Furthermore, the computational calculation of the K_2O-CaO-SiO_2 phase diagram published in the literature is from Kim [23] and Zhang et al. [24] only. The compounds mostly found by Morey at al. [1,2] were included in their assessments. Although Kim [23] was aware that $K_2O{\cdot}CaO{\cdot}SiO_2$ was reported to be absent by Arroyabe et al. [17] and Bankole et al. [18], they [23,24] still included this compound in the parameter estimation and as a result, the primary phase field of $K_2O{\cdot}CaO{\cdot}SiO_2$ is still seen in the computed ternary diagram. Zhang et al. used Thermocalc [24] and only reported the primary phase field boundaries of the ternary system in terms of univariant lines. The insufficient experimental data in the system limits the calculation result. Moreover, recently a new compound, $K_2O{\cdot}3CaO{\cdot}3SiO_2$ synthesized at high pressure was reported by Arroyabe et al. [25] and is also stable at 1 atm, as reported by Schmidmair et al. [26,27], who also found a new compound $K_2O{\cdot}CaO{\cdot}4SiO_2$. Thus, inclusion of these two new compounds in the calculation will affect the results of the previous critical assessments.

Challenge in the experimental investigation of K_2O-CaO-SiO_2 phase equilibria is potassia evaporation from the samples during equilibration. If chemical analysis is carried out before the equilibration, in which evaporation of potassia is taking place, then the true liquid compositions do not represent those of the initial mixtures. This can be the reason of the notable systematic shifting of liquidus lines reported by Morey et al. [1] compared to the data obtained by Chen et al. [19], especially at high potassium concentration areas at $CaO{\cdot}SiO_2$ and $K_2O{\cdot}2CaO{\cdot}2SiO_2$ saturations. Morey [1,2] used pre equilibration chemical analysis. The presence of phases at high temperatures quenched in cold water was examined under optical microscope. Because potassia was evaporating during equilibration process, the reported liquidus will be higher in K_2O content than the actual one. By the using Equilibration-Quenching-EPMA method employed by Chen et al. [19], evaporation will not affect the results because chemical analysis was carried out after evaporation of K_2O i.e. after the equilibrium was achieved. In the present study, Equilibration-Quenching-EPMA/EDS technique was employed to revisit the measurements done by previous authors and to generate data that has not found to be published. A comparison between the EPMA and EDS analyses was also made. Phase relations of the liquid at different primary phase fields and temperatures will be reported as isothermal sections and liquidus projections. Once the fully liquid boundaries in the ternary system were obtained, viscosity calculation of the molten mixtures were undertaken. In the present investigation, temperature and ash composition regions that are suitable from a slag flow perspective in the entrained flow gasifier will also be presented.

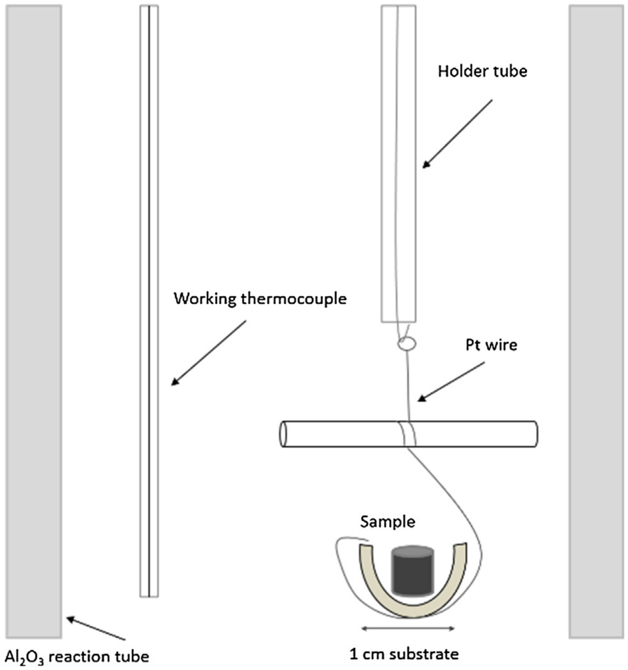

Fig. 1. Sample container design.

2. Methodology

2.1. Experimental technique

Equilibration of the samples at high temperatures followed by quenching in an ice cold water and chemical analysis of the quenched phases by EPMA [28] and EDS were used to investigate K_2O-CaO-SiO_2 system in the present study. Initial mixtures of 0.15 g made from high purity K_2CO_3, CaO and SiO_2 powders were pressed to form a pellet. The samples were then placed in a container. The containers used in the present study were pure platinum foil or fused SiO_2, depending on the primary phase present at equilibrium. The design of the crucible is presented in Fig. 1.

The top of the furnace was installed with a brass water-cooled head that had two holes for sample holder and thermocouple insertion. The head was also connected to a water cooled shield. The samples were equilibrated by hanging them in the isothermal hot zone of the work tube by a 0.5 mm platinum wire. The samples were equilibrated in air by opening the top and the bottom of the furnace to the ambient atmosphere. A schematic design of the vertical tube furnace is presented in Fig. 2. The furnace was heated with SiC heating elements and its temperature was measured by a calibrated S type thermocouple made from Pt-10 wt% Rh and pure platinum wires (Johnson-Matthey, UK). The thermocouple placed close to the sample was attached to a 2000 multimeter (Keithley, USA) that was connected to NI LabView computer program to continuously record temperature inside the furnace every 5 s. Overall temperature measurement accuracy of ± 2 °C was obtained.

After equilibrium was attained, the phases present in the sample at high temperatures were preserved by quenching it by pulling the sample holder upward so that the samples dropped quickly to the cooled water. The samples were dried by hot air flush to remove the traces of quenching water in the samples and then mounted in an epoxy resin. Dry polishing technique was employed. The samples were carbon coated and sent for EDS and EPMA analysis. There was no difficulty to retain the homogeneous equilibrium phases by quenching. The liquid phase can be preserved as a homogeneous glassy phase and the solid phases remained unchanged.

The achievement of equilibrium was examined as follows: 1.) By

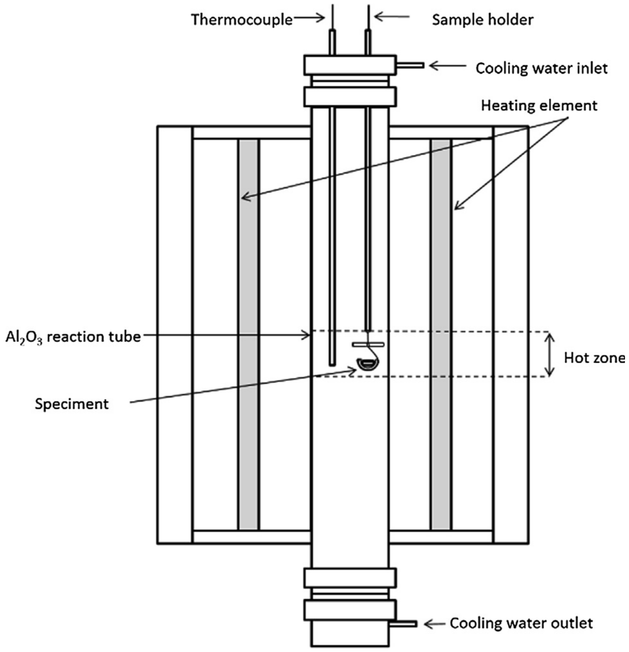

Fig. 2. Furnace arrangement.

Table.1
Chemical used in the experiments.

Compounds	Purity (wt%)	Supplier
SiO_2	99.99	Umicore
K_2CO_3	99.5	Sigma Aldrich
CaO	99.9	Sigma Aldrich
$CaO{\cdot}SiO_2$	99	Alfa Aesar

equilibrating the samples at different holding times. In the present study, experiments were carried out with duration from 4.5 to 165 h. The samples confirmed to have reached equilibrium at certain time if concentrations of the phases obtained from experiment at different holding times remained the same; 2.) By approaching the equilibrium from different compounds. To obtain the same equilibrium position, different starting materials were used. For example, a ternary liquidus point was not only approached by using $CaO{\cdot}SiO_2$ and $K_2O{\cdot}SiO_2$ mixtures but also using CaO, K_2CO_3 or $K_2O{\cdot}SiO_2$ and SiO_2 mixtures to ensure that the phases were formed by chemical reaction at a high temperature. The purities and suppliers of the chemicals are presented in Table 1; 3.) By approaching the equilibrium from two different directions. To obtain the same equilibrium point, the samples were equilibrated directly at the selected temperature and also pre-melted by which the sample were heated to the temperatures above the targeted temperature for several hours and then cooled down to the targeted temperature and equilibrated for selected period of time. The results approached from two different directions must be the same when the equilibrium is attained; 4.) By evaluating the homogeneity of the phases by using EPMA (Cameca SX100) and EDS (Tescan Mira3) to ensure that there are no concentration gradients and to ensure the location of analysis was correct especially at double solid saturations at which the liquid have to touch both crystals.

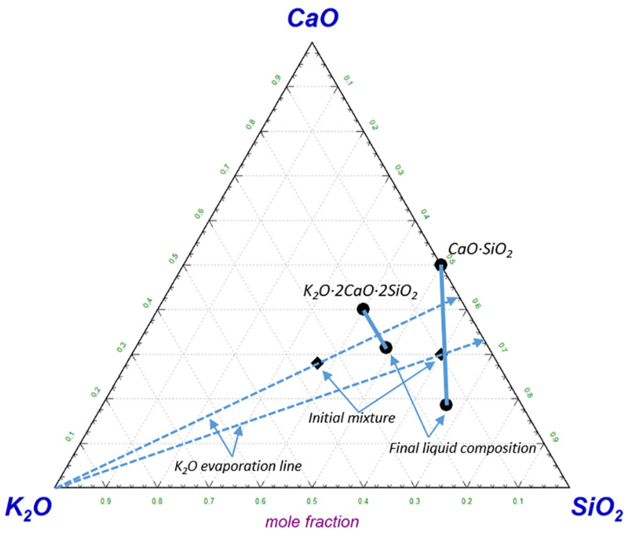

Fig. 3. Paths of compositional changing of the equilibrated mixtures at 1200 °C for 5 h.

During the EDS and EPMA analyses, appropriate measurement parameters were selected to avoid the depletion of potassium caused by the electron beam. For EPMA measurements, accelerating voltage of 20 kV, beam current of 20 nA and diameter of 1 μm were employed. Astimex diopside ($MgCaSi_2O_6$) and sanidine ((K, Na)(Si, Al)$_4$O$_8$) were used for Si, Ca and K standards, respectively. For EDS analysis, 15 kV accelerating voltage, 420 nm spot size and area of 100–200 μm^2 (instead of point) analysis were used. Sanidine, calcite and quartz were used as external K, Ca and Si standards, respectively. ZAF correction were employed for both analyses. The EDS and EPMA analysis results of the stoichiometric compounds were compared with their true theoretical values presented in Table 2.

It can be seen in Table 2 that there is a good agreement between the stoichiometric formula values and the EDS and EPMA results with the accuracy around 1 mol%. It means that the compositional analyses of the quenched samples by using EDS were reliable. This also agreed with result from Akdogan et al. [29] who reported that EDS analysis were applicable for analyzing K_2O-SiO_2 glass after a carefully made comparison with the corresponding EPMA analysis. In the present study, the unknown liquids composition were measured together with the known compositions of solid phases precipitated in the liquid during EDS analysis. The analysis result of the solid phase are presented together with the result of the liquidus measurement. The accuracy of the analysis can be confirmed from the result of the known composition of solid phase. For each compositional data of each phase, five areas of EDS analysis were undertaken at homogenous phases with the obtained

Table 2
Results of EDS and EPMA analyses comparing the stoichiometric compounds.

Crystal	Theoretical value (mol%)			EDS Analysis (mol%)			EPMA Analysis (mol%)		
	CaO	K_2O	SiO_2	CaO	K_2O	SiO_2	CaO	K_2O	SiO_2
$CaO{\cdot}SiO_2$	50.0	0	50.0	49.0	0	51.0	49.9	0	50.1
$3CaO{\cdot}2SiO_2$	60.0	0	40.0	58.9	0	41.1	59.9	0	40.1
$2CaO{\cdot}SiO_2$	66.7	0	33.3	65.4	0	34.6	66.4	0	33.6
$K_2O{\cdot}3CaO{\cdot}3SiO_2$	42.9	14.3	42.8	41.9	14.6	43.5	42.5	14.0	43.5
$K_2O{\cdot}6CaO{\cdot}4SiO_2$	54.6	9.1	36.3	53.8	9.1	37.0	54.3	8.9	36.8
$K_2O{\cdot}2CaO{\cdot}2SiO_2$	40.0	20.0	40.0	38.8	20.5	40.8	39.4	19.9	40.6

Table 3
Chemical compositions of the quenched phases.

Sample No	Temperature (°C)	Equilibration time (h)	Phases	Chemical Composition (mol %)		
				K_2O	CaO	SiO_2
KCS-211	800	165	SiO_2	0	0	100
			Liquid	18.0	0	82.0
KCS-113	900	141.5	SiO_2	0	0	100
			Liquid	17.8	0	82.2
KCS-174	1000	46	SiO_2	0	0	100
			Liquid	16.1	0	83.9
KCS-46	1000	52.5	SiO_2	0	0	100
			Liquid	11.9	7.2	80.9
KCS-47	1000	52.5	*SiO2*	0	0	100
			$CaO{\cdot}SiO_2$	0	47.6	52.4
			Liquid	10.1	11.0	78.9
KCS-57	1000	41	$CaO{\cdot}SiO_2$	0	48.8	51.2
			Liquid	13.6	12.3	74.1
KCS-42	1000	51	$CaO{\cdot}SiO_2$	0	48.9	51.1
			Liquid	15.5	13.3	71.2
KCS-41	1000	51	$CaO{\cdot}SiO_2$	0	49.2	50.8
			Liquid	19.8	14.5	65.7
KCS-53	1000	51.5	$CaO{\cdot}SiO_2$	0	48.6	51.4
			Liquid	22.5	16.1	61.4
KCS-105	1000	67	$CaO{\cdot}SiO_2$	0	48.8	51.2
			Liquid	22.9	16.7	60.4
KCS-107	1000	67	$CaO{\cdot}SiO_2$	0	48.8	51.2
			Liquid	23.3	17.7	59.0
KCS-102	1000	67	$CaO{\cdot}SiO_2$	0	48.7	51.3
			Liquid	23.4	18.5	58.1
KCS-56, 96, 97, 98, 100, 101, 103, 214, 215, 216	1000	66.4	$CaO{\cdot}SiO_2$	0	48.8	51.2
			$K_2O{\cdot}2CaO{\cdot}2SiO_2$	20.5	38.5	41.0
			Liquid	23.0	21.2	55.8
KCS-44	1000	45	$K_2O{\cdot}2CaO{\cdot}2SiO_2$	21.1	38.2	40.7
			Liquid	29.1	15.0	55.9
KCS-187	1000	66	$K_2O{\cdot}2CaO{\cdot}2SiO_2$	19.6	38.8	41.6
			Liquid	30.9	13.7	55.4
KCS-188	1000	66	$K_2O{\cdot}2CaO{\cdot}2SiO_2$	20.8	38.6	40.6
			Liquid	31.8	13.0	55.2
KCS-175	1100	94	SiO_2	0	0	100
			Liquid	14.9	0	85.1
KCS-60	1100	26.5	SiO_2	0	0	100
			Liquid	11.8	4.9	83.3
KCS-401	1100	26.5	SiO_2	0	0	100
			$CaO{\cdot}SiO_2$	0	48.4	51.6
			Liquid	8.9	12.5	78.6
KCS-68	1100	26	$CaO{\cdot}SiO_2$	0	48.3	51.7
			Liquid	15.1	15.2	69.7
KCS-67	1100	26	$CaO{\cdot}SiO_2$	0	48.7	51.3
			Liquid	18.3	16.8	64.9
KCS-63	1100	26.5	$CaO{\cdot}SiO_2$	0.0	48.9	51.1
			Liquid	19.1	17.6	63.3
KCS-117	1100	46.5	$CaO{\cdot}SiO_2$	0	49.1	50.9
			Liquid	20.3	20.7	59.0
KCS-118	1100	46.5	$CaO{\cdot}SiO_2$	0	49.5	50.5
			Liquid	19.8	22.7	57.5
KCS-233	1100	43	$CaO{\cdot}SiO_2$	0	48.9	51.1
			Liquid	19.6	25.6	54.8
KCS-69, 114, 115, 119	1100	46.5	$CaO{\cdot}SiO_2$	0	49.2	50.8
			$3CaO{\cdot}2SiO_2$	0	58.9	41.1
			Liquid	19.2	26.9	53.9
KCS-141	1100	25	$2CaO{\cdot}SiO_2$	0	64.7	35.3
			$K_2O{\cdot}6CaO{\cdot}4SiO_2$	8.8	53.9	37.3
			Liquid	17.8	30.1	52.1
KCS-220	1100	43	$K_2O{\cdot}6CaO{\cdot}4SiO_2$	9.0	54.2	36.8
			Liquid	19.0	29.4	51.6
KCS-306	1100	50	$K_2O{\cdot}6CaO{\cdot}4SiO_2$	9.0	54.2	36.8
			Liquid	18.0	30.9	51.1
KCS-195	1100	52	$K_2O{\cdot}6CaO{\cdot}4SiO_2$	9.2	53.6	37.2
			$K_2O{\cdot}2CaO{\cdot}2SiO_2$	20.3	39.0	40.7
			Liquid	20.3	28.3	51.4
KCS-194	1100	52	$K_2O{\cdot}2CaO{\cdot}2SiO_2$	20.5	39.1	40.4
			Liquid	22.7	25.2	52.1
KCS-176	1200	38	*SiO2*	0	0	100
			Liquid	13.3	0	86.7
KCS-14	1200	12	SiO_2	0	0	100
			Liquid	11.8	3.0	85.2

(*continued on next page*)

Table 3 (*continued*)

Sample No	Temperature (°C)	Equilibration time (h)	Phases	Chemical Composition (mol %)		
				K_2O	CaO	SiO_2
KCS-1	1200	5	SiO_2	0	0	100
			Liquid	11.0	5.3	83.7
KCS-404	1200	22	SiO_2	0	0	100
			$CaO\cdot SiO_2$	0	48.6	51.4
			Liquid	7.4	14.5	78.1
KCS-28	1200	12.5	$CaO\cdot SiO_2$	0	48.9	51.1
			Liquid	11.3	17.3	71.4
KCS-408	1200	22	$CaO\cdot SiO_2$	0	48.1	51.9
			Liquid	12.9	18.5	68.6
KCS-3	1200	5	$CaO\cdot SiO_2$	0	48.1	51.9
			Liquid	14.7	18.5	66.8
KCS-180	1200	34	$CaO\cdot SiO_2$	0	49.5	50.5
			Liquid	16.9	20.9	62.2
KCS-19	1200	6	$CaO\cdot SiO_2$	0	49.3	50.7
			Liquid	18.0	21.9	60.1
KCS-22	1200	11.5	$CaO\cdot SiO_2$	0	49.1	50.9
			Liquid	17.4	25.7	56.9
KCS-182	1200	34	$CaO\cdot SiO_2$	0	48.6	51.4
			Liquid	16.9	27.8	55.3
KCS-21, 183	1200	34	$CaO\cdot SiO_2$	0	49.1	50.9
			$3CaO\cdot 2SiO_2$	0	59.0	41.0
			Liquid	15.8	32.1	52.1
KCS-208	1200	26	$3CaO\cdot 2SiO_2$	0	58.6	41.4
			Liquid	16.0	32.4	51.6
KCS-11	1200	4.5	$2CaO\cdot SiO_2$	0	65.5	34.5
			Liquid	14.6	35.2	50.2
KCS-204	1200	24.5	$2CaO\cdot SiO_2$	0	65.3	34.7
			Liquid	17.3	32.6	50.1
KCS-10	1200	4.5	$K_2O\cdot 6CaO\cdot 4SiO_2$	9.3	53.9	36.8
			Liquid	19.9	30.6	49.5
KCS-26	1200	5	$K_2O\cdot 6CaO\cdot 4SiO_2$	9.4	53.6	37.0
			$K_2O\cdot 2CaO\cdot 2SiO_2$	20.7	38.7	40.6
			Liquid	20.4	30.7	48.9
KCS-31	1200	5	$K_2O\cdot 2CaO\cdot 2SiO_2$	20.4	39.2	40.4
			Liquid	22.9	27.4	49.7
KCS-177	1300	23	SiO_2	0	0	100
			Liquid	11.5	0	88.5
KCS-254	1300	12	SiO_2	0	0	100
			Liquid	8.7	6.5	84.8
KCS-253	1300	12	SiO_2	0	0	100
			Liquid	7.8	9.7	82.5
KCS-398	1300	21.5	SiO_2	0	0	100
			$CaO\cdot SiO_2$	0	48.8	51.2
			Liquid	5.5	17.9	76.6
KCS-401	1300	21.5	$CaO\cdot SiO_2$	0	49.8	50.2
			Liquid	7.2	20.2	72.6
KCS-402	1300	21.5	$CaO\cdot SiO_2$	0	49.6	50.4
			Liquid	7.9	21.0	71.1
KCS-330	1300	6	$CaO\cdot SiO_2$	0	49.4	50.6
			Liquid	8.7	21.5	69.8
KCS-329	1300	6	$CaO\cdot SiO_2$	0	49.2	50.8
			Liquid	10.4	22.3	67.3
KCS-257	1300	12	$CaO\cdot SiO_2$	0	49.4	50.6
			Liquid	12.0	23.1	64.9
KCS-328	1300	6	$CaO\cdot SiO_2$	0	49.2	50.8
			Liquid	12.6	24.8	62.6
KCS-152	1300	20	$CaO\cdot SiO_2$	0	48.5	51.5
			Liquid	13.3	26.8	59.9
KCS-81	1300	18	$CaO\cdot SiO_2$	0	49.2	50.8
			Liquid	13.2	28.1	58.7
KCS-78	1300	18	$CaO\cdot SiO_2$	0	49.0	51.0
			Liquid	13.6	30.6	55.8
KCS-83	1300	18	$CaO\cdot SiO_2$	0	49.2	50.8
			Liquid	12.9	33.4	53.7
KCS-243	1300	24	$CaO\cdot SiO_2$	0.0	49.1	50.9
			Liquid	11.7	36.7	51.6
KCS-130, 131	1300	45.5	$CaO\cdot SiO_2$	0	48.7	51.3
			$3CaO\cdot 2SiO_2$	0	58.5	41.5
			Liquid	10.3	40.0	49.7
KCS-335	1300	8	$3CaO\cdot 2SiO_2$	0	59.1	40.9
			Liquid	9.2	42.0	48.8
KCS-332	1300	8	$2CaO\cdot SiO_2$	0	66.0	34.0
			Liquid	6.7	45.7	47.6

(*continued on next page*)

Table 3 (*continued*)

Sample No	Temperature (°C)	Equilibration time (h)	Phases	Chemical Composition (mol %)		
				K_2O	CaO	SiO_2
KCS-340	1300	18	$2CaO\cdot SiO_2$	0	65.8	34.2
			Liquid	9.2	43.5	47.3
KCS-308	1300	6	$2CaO\cdot SiO_2$	1.4	64.0	34.6
			Liquid	12.3	40.4	47.3
KCS-310	1300	6	$2CaO\cdot SiO_2$	1.5	63.8	34.7
			Liquid	13.3	39.5	47.2
KCS-379	1300	4	$2CaO\cdot SiO_2$	1.8	63.6	34.6
			Liquid	16.0	36.9	47.1
KCS-377	1300	4	$2CaO\cdot SiO_2$	1.9	63.6	34.5
			Liquid	17.4	35.7	46.9
KCS-178	1400	5	SiO_2	0	0	100
			Liquid	9.4	0	90.6
KCS-162	1400	12	SiO_2	0	0	100
			Liquid	5.7	8.9	85.4
KCS-163	1400	12	SiO_2	0	0	100
			Liquid	4.7	15.0	80.3
KCS-394	1400	18	SiO_2	0.0	0.0	100
			Liquid	3.6	21.9	74.5
KCS-397	1400	18	SiO_2	0	0	100
			Liquid	3.0	24.4	72.6
KCS-392	1400	18	SiO_2	0	0	100
			Liquid	2.7	26.4	70.9
KCS-393	1400	18	SiO_2	0	0	100
			$CaO\cdot SiO_2$	0	48.9	51.1
			Liquid	2.5	29.1	68.4
KCS-366	1400	12	$CaO\cdot SiO_2$	0	49.1	50.9
			Liquid	5.9	29.2	64.9
KCS-364	1400	12	$CaO\cdot SiO_2$	0	49.3	50.7
			Liquid	6.9	30.0	63.2
KCS-321	1400	6	$CaO\cdot SiO_2$	0	49.3	50.7
			Liquid	6.9	32.8	60.2
KCS-167	1400	7	$CaO\cdot SiO_2$	0	49.9	50.1
			Liquid	7.5	33.4	59.1
KCS-389	1400	22.5	$CaO\cdot SiO_2$	0	49.4	50.6
			Liquid	7.3	42.1	50.6
KCS-319	1400	7	$CaO\cdot SiO_2$	0	49.5	50.5
			Liquid	7.5	35.7	56.8
KCS-171	1400	7	$CaO\cdot SiO_2$	0	48.9	51.1
			Liquid	7.9	40.0	52.1
KCS-173	1400	7	$CaO\cdot SiO_2$	0	49.1	50.9
			Liquid	5.7	45.8	48.6
KCS-260	1400	7	$CaO\cdot SiO_2$	0	48.9	51.1
			$3CaO\cdot 2SiO_2$	0	59.0	41.0
			Liquid	4.7	48.6	46.7
KCS-262	1400	7	$3CaO\cdot 2SiO_2$	0	59.0	41.0
			Liquid	4.3	49.1	46.6
KCS-261	1400	7	$2CaO\cdot SiO_2$	0	65.1	34.9
			Liquid	3.0	51.2	45.8
KCS-262-2	1400	7	$2CaO\cdot SiO_2$	0	65.2	34.8
			Liquid	3.7	50.1	46.2
KCS-356	1400	5.5	$2CaO\cdot SiO_2$	0.7	64.9	34.4
			Liquid	5.2	49.2	45.6
KCS-358	1400	5.5	$2CaO\cdot SiO_2$	0.7	64.8	34.5
			Liquid	5.8	48.5	45.7
KCS-345	1400	6	$2CaO\cdot SiO_2$	1.0	64.6	34.4
			Liquid	7.9	46.1	46.0
KCS-347	1400	6	$2CaO\cdot SiO_2$	1.1	64.4	34.5
			Liquid	8.6	45.3	46.1
KCS-373	1400	4	$2CaO\cdot SiO_2$	1.4	63.9	34.7
			Liquid	11.8	42.2	46.0
KCS-185	1500	5	SiO_2	0	0.0	100
			Liquid	5.1	0.0	94.9

standard deviations of less than ± 0.1 mol%.

2.2. *Thermodynamic and viscosity calculation*

In the present investigation thermodynamic calculation to obtain phase diagrams were undertaken by FactSage version 7.3, using the FTOxid database [22] and also by MTDATA [20] using Mtox vers. 8.2 database [21]. For the viscosity calculations, the viscosity model available in the Factsage 7.3 [22] was employed. The viscosity model has been reported previously by Grundy et al. [30]. Thermodynamic calculations by FactSage [22] and MTDATA [20] were compared with the experimental data obtained in the present study. Viscosity calculation are superimposed with the liquidus boundaries obtained in the present investigation.

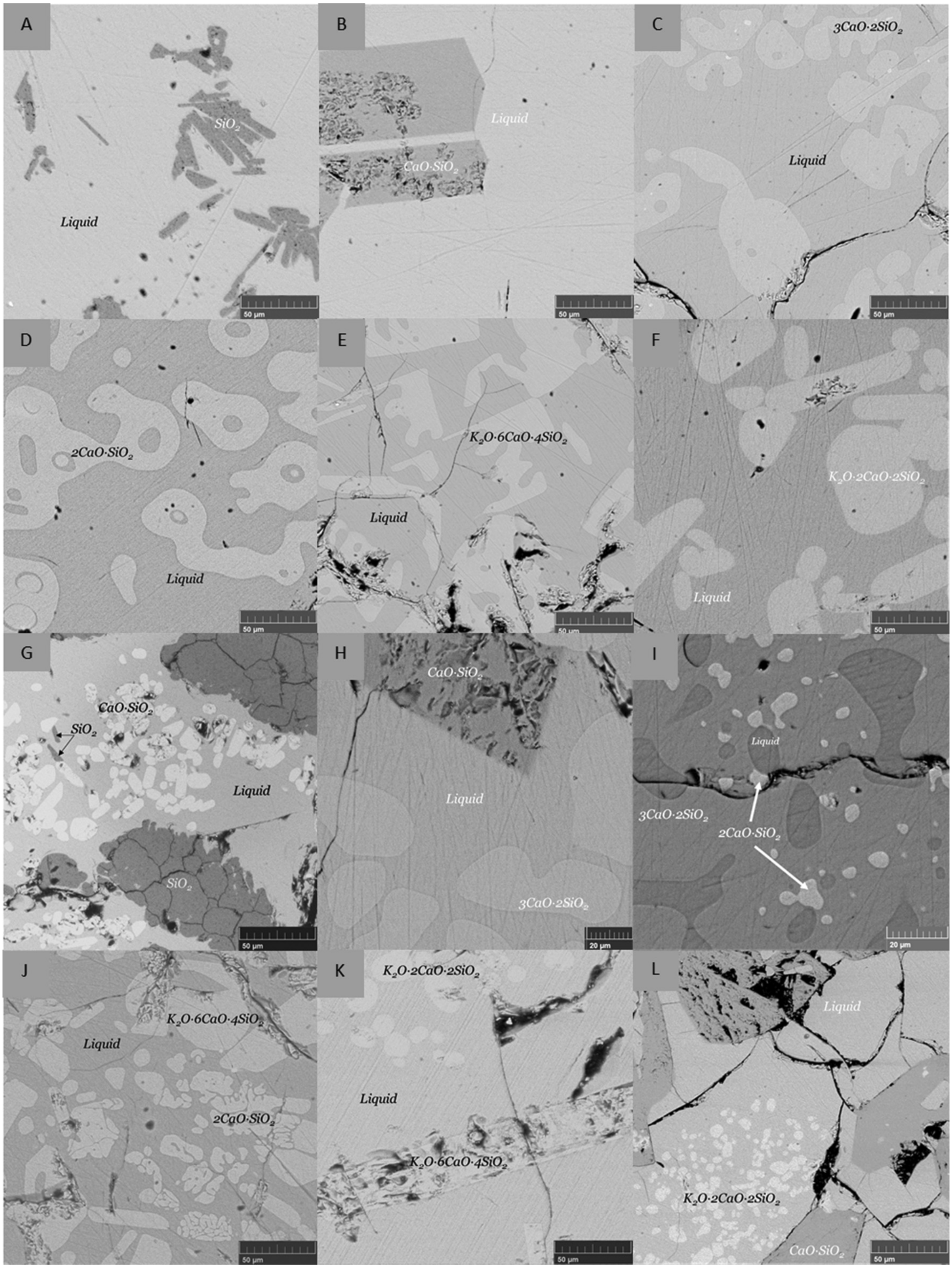

Fig. 4. Backscattered electron images of quenched samples representing the phase relations of the liquid with: A. SiO_2; B. $CaO·SiO_2$; C. $3CaO·2SiO_2$; D. $2CaO·SiO_2$; E. $K_2O·6CaO·4SiO_2$; F. $K_2O·2CaO·2SiO_2$; G. SiO_2 + $CaO·SiO_2$; H. $CaO·SiO_2$ + $3CaO·2SiO_2$; I. $3CaO·2SiO_2$ + $2CaO·SiO_2$; J. $2CaO·SiO_2$ + $K_2O·6CaO·4SiO_2$; K. $K_2O·6CaO·4SiO_2$ + $K_2O·2CaO·2SiO_2$; L. $CaO·SiO_2$ + $K_2O·2CaO·2SiO_2$.

3. Result and discussion

3.1. *Behavior of K_2O during experiment*

By using this technique to investigate ternary system, the evaporation not only changes the proportion of liquid and solid phases but also does change the location of tie line from the initial mixture in a ternary system. Therefore, a failure to select appropriate initial mixture will end up with an unwanted equilibrium position and phase assemblages. Fig. 3 shows the theoretical evaporation paths of K_2O from two different initial mixtures that extend from the K_2O corner, crossing the initial bulk compositions to the $CaO\text{-}SiO_2$ direction. It can be seen from Fig. 3 that for equilibration of initial mixture contains 35 mol% K_2O at 1200 °C for 5 h, the final K_2O concentration in the liquid was 20 mol%

Table 4
Phase relations in the K_2O-CaO-SiO_2 system obtained in the present study.

Phase Relation	Microstructure
Liquid + SiO_2	Fig. 4A
Liquid + $CaO{\cdot}SiO_2$	Fig. 4B
Liquid + $3CaO{\cdot}2SiO_2$	Fig. 4C
Liquid + $2CaO{\cdot}SiO_2$	Fig. 4D
Liquid + $K_2O{\cdot}6CaO{\cdot}4SiO_2$	Fig. 4E
Liquid + $K_2O{\cdot}2CaO{\cdot}2SiO_2$	Fig. 4F
Liquid + SiO_2 + $CaO{\cdot}SiO_2$	Fig. 4G
Liquid + $CaO{\cdot}SiO_2$ + $3CaO{\cdot}2SiO_2$	Fig. 4H
Liquid + $3CaO{\cdot}2SiO_2$ + $2CaO{\cdot}SiO_2$	Fig. 4I
Liquid + $2CaO{\cdot}SiO_2$ + $K_2O{\cdot}6CaO{\cdot}4SiO_2$	Fig. 4J
Liquid + $K_2O{\cdot}6CaO{\cdot}4SiO_2$ + $K_2O{\cdot}2CaO{\cdot}2SiO_2$	Fig. 4K
Liquid + $CaO{\cdot}SiO_2$ + $K_2O{\cdot}2CaO{\cdot}2SiO_2$	Fig. 4L

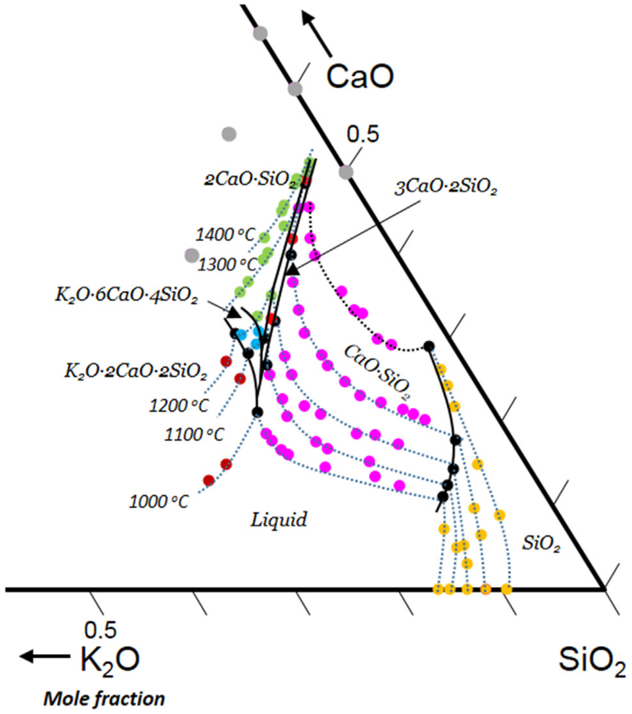

Fig. 5. Liquidus projections of the K_2O-CaO-SiO_2 system and its primary phase fields.

and it was located on the tie line with $K_2O{\cdot}2CaO{\cdot}2SiO_2$. It means that 10 mol% of K_2O was evaporated.

However, if the K_2O concentration in the initial bulk mixture is 10 mol%, this initial bulk composition remains located in the tie line between the final liquidus composition and the solid phase which is $CaO{\cdot}SiO_2$ meaning that evaporation is negligible at this condition. Therefore, by understanding the behavior of K_2O, certain initial mixture can be selected for obtaining the specific equilibrium assemblage. The final equilibrium compositions of the phases analyzed by EDS are presented in Table 3. The backscattered electron images of quenched phases at different primary phase fields are presented in Fig. 4.

3.2. Phase relations

In the present study, 12 types of phase relations presented in Table 4 were obtained and their microstructures are presented in Fig. 4A–L. The liquidus composition data in Table 3 are presented in Fig. 5 as a liquidus projection from 1000 to 1400 °C at different primary phase fields to give a general overview of the suggested liquidus contours of the K_2O-CaO-SiO_2 ternary diagram based on the data obtained in the present study. To see the phase relations between each phase in more detail, the data were also plotted as isothermal sections in Fig. 6A–E for temperatures of 1000–1400 °C, respectively.

The binary data obtained in the present study compared with the previous investigation [29] and assessed phase diagram by FactSage using FTOxid vers. 7.3 database [22] is presented in Fig. 7. A comparison of ternary experimental data obtained in the present study with that obtained by Chen et al. [19] are presented in Figs. 8–11 along with the assessed phase diagram by MTDATA [20] using Mtox vers. 8.2 database [21] and FactSage [22] at 1000 and 1100 °C, respectively.

As can been seen in Fig. 5, there are 6 primary phase fields obtained in the present study surrounding the liquid phase which are primary phase fields of SiO_2, $CaO{\cdot}SiO_2$, $3CaO{\cdot}2SiO_2$, $2CaO{\cdot}SiO_2$, $K_2O{\cdot}6CaO{\cdot}4SiO_2$ and $K_2O{\cdot}2CaO{\cdot}2SiO_2$. Each primary phase field cuts each other along the univariant line drawn as a solid line and black point in the diagram in Fig. 5.

3.3. Primary phase field of SiO_2

It can be seen in Fig. 7 that the liquidus compositions of the SiO_2 primary phase field in the binary K_2O-SiO_2 system obtained in the present study are in a good agreement with the data reported by Morey [1] and also calculated phase diagram by FactSage [22]. The data by Akdogan et al. [29] at 800, 900 and 1000 °C are in a poor agreement with those obtained in the present investigation because their data are located in the fully liquid area of the present study. Moreover, the microstructures at 1000 °C reported by Akdogan et al. [29] seems to be fully liquid microstructure since there is no secondary SiO_2 precipitates inside the liquid phase to ensure that the liquid composition is in equilibrium with $SiO_{2,}$ although the crucible used was SiO_2. As can be seen in Figs. 8 and 9, at 1000 and 1100 °C, respectively, the ternary liquidus composition at SiO_2 saturation data obtained in the present study are in a good agreement with the data reported by Chen et al. [19] and the calculated phase diagram by MTDTA [20,21] at 1100 °C (Fig. 9). However, FactSage [22] calculated liquidus compositions seem to have higher K_2O concentrations, especially when the overall composition is located close to the saturation of $CaO{\cdot}SiO_2$, as can be seen in Figs. 10 and 11.

3.4. Primary phase field of $CaO{\cdot}SiO_2$

The liquidus compositions at $CaO{\cdot}SiO_2$ saturation at 1000 and 1100 °C are in a good agreement with the data reported by Chen et al. [19] and with the calculated phase diagram by FactSage [22] (Figs. 10 and 11). However, at 1000 and 1100 °C and at low K_2O concentrations, MTDATA [20,21] showed saturation of the liquidus with $K_2O{\cdot}2CaO{\cdot}9SiO_2$ and $K_2O{\cdot}3CaO{\cdot}6SiO_2$ as shown in Figs. 8 and 9. These two ternary compounds were not observed in the present investigation near to $CaO{\cdot}SiO_2$ saturation at 1000 and 1100 °C.

The $CaO{\cdot}SiO_2$ primary phase field intersects the SiO_2 primary phase field at a univariant line that was previously only predicted by extrapolation by Morey et al. [1] and Chen et al. [19]. However, in the present study, a liquid at double crystal saturations of $CaO{\cdot}SiO_2$ and SiO_2 (Fig. 4G) was determined for the first time in the temperature range from 1000 to 1400 °C and therefore the exact location of the intersection between the $CaO{\cdot}SiO_2$ and SiO_2 primary phase fields is now known by experimentation. According to the calculation by MTDATA [20,21] (Fig. 9) and FactSage [22] (Fig. 11) at 1100 °C, the liquidus composition at this double solid saturations has a slightly higher CaO concentration than the experimental data obtained in the present study

3.5. Primary phase field of $3CaO{\cdot}2SiO_2$

There has been no experimental data previously reported to support the stability of a liquid with the $3CaO{\cdot}2SiO_2$ primary phase in the ternary system. Morey at al. [1] predicted only the existence of the primary phase field to be very narrow and it disappeared at around

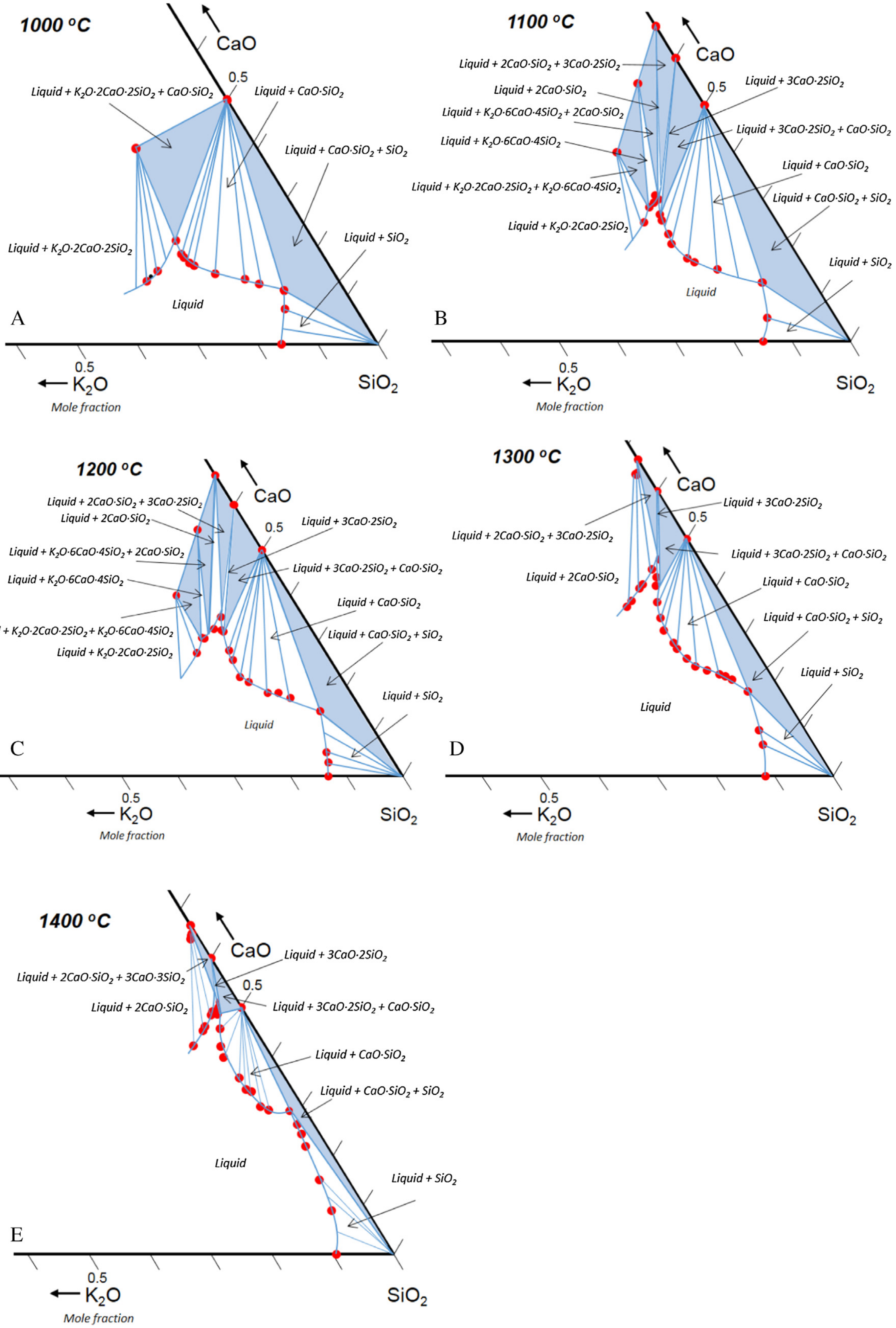

Fig. 6. Isothermal section of the K_2O-CaO-SiO_2 system at: A. 1000 °C, B. 1100 °C, C. 1200 °C, D. 1300 °C, E. 1400 °C.

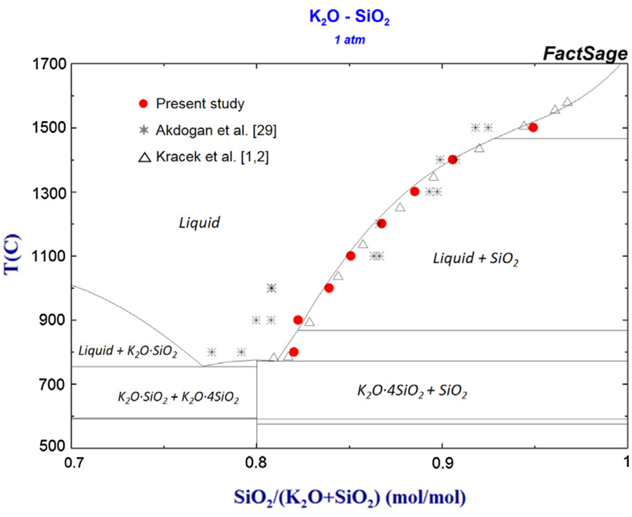

Fig. 7. Binary K_2O-SiO_2 phase diagram [22].

1400 °C upon cooling. However, in the present study not only the liquid in equilibrium with $3CaO·2SiO_2$ (Fig. 4C) was obtained but also the liquid composition in equilibrium with two solid compounds of $3CaO·2SiO_2$ and $CaO·SiO_2$ (Fig. 4H) between 1100 and 1400 °C. It means that the exact location of the intersection between $3CaO·2SiO_2$ and $CaO·SiO_2$ primary phase fields are now known by experimentation between 1100 and 1400 °C. It can be seen in Fig. 6B–E, that the $3CaO·2SiO_2$ primary phase field is very narrow, as also reproduced by MTDATA [20,21] (Fig. 9) and FactSage [22] (Fig. 11). According to calculated phase diagram by MTDATA [20,21] (Fig. 8) and Factsage [22] (Fig. 10) this primary was still stable at 1000 °C. However, present investigation showed a different behavior. As can be seen in Fig. 6A, at 1000 °C the primary phase field of $CaO·SiO_2$ intersects the primary phase field of $K_2O·2CaO·SiO_2$ (the data from experiments of 10 samples: KCS-56, 96, 97, 98, 100, 101, 103, 214, 215, 216) meaning that there is no space for the $3CaO·2SiO_2$ primary phase in equilibrium with the liquid oxide.

3.6. Primary phase field of $2CaO·SiO_2$

From Fig. 5 it can be seen that between 1000 and 1100 °C the primary phase field of $2CaO·SiO_2$ is relatively narrow. However, it becomes wider at higher temperatures. Data by Chen et al. [19] are in a good agreement with those obtained in the present investigation. Between 1300 and 1400 °C, $2CaO·SiO_2$ can dissolve considerable fraction of K_2O up to 1.9 at%. This agrees with the prediction by Morey et al. [1] about the solubility of K_2O in $2CaO·SiO_2$ that was also proven by Suzukawa [31], Fedorov and Brodkina [32] who reported a $2CaO·SiO_2$ solid solution. According to calculation by Kim [23], the $2CaO·SiO_2$ primary phase field disappeared upon cooling at 1290 °C through a peritectic reaction of $L + 2CaO·SiO_2 \leftrightarrow 3CaO·2SiO_2 + K_2O·6CaO·4SiO_2$. Therefore, the calculated diagram by FacSage [23,22] (Fig. 11) showed that at 1100 °C the liqudus line at $2CaO·SiO_2$ saturation was absent. However, data obtained in the present study indicated that at 1100 °C $2CaO·SiO_2$ can be in equilibrium with the liquid phase as also predicted by MTDATA [20,21] (Fig. 9). It was difficult to obtain liquidus data in the double saturation of $2CaO·SiO_2$ and $3CaO·2SiO_2$ where a liquid is in contact with both compounds. As can be seen in Fig. 4I, most of the $2CaO·SiO_2$ were precipitated inside $3CaO·2SiO_2$ crystals. If there was a liquid in contact with both crystals to ensure its double saturation, the liquid area was limited and very small to be measured, as also indicated in Fig. 4I.

3.7. Primary phase field $K_2O·6CaO·4SiO_2$

The data obtained by Chen et al. [19] at $K_2O·6CaO·4SiO_2$ saturation at 1100 °C is in a good agreement with the present study. However, at 1100 °C calculated phase diagram by FactSage [22] indicated that the liquidus boundaries have a lower CaO concentration since the

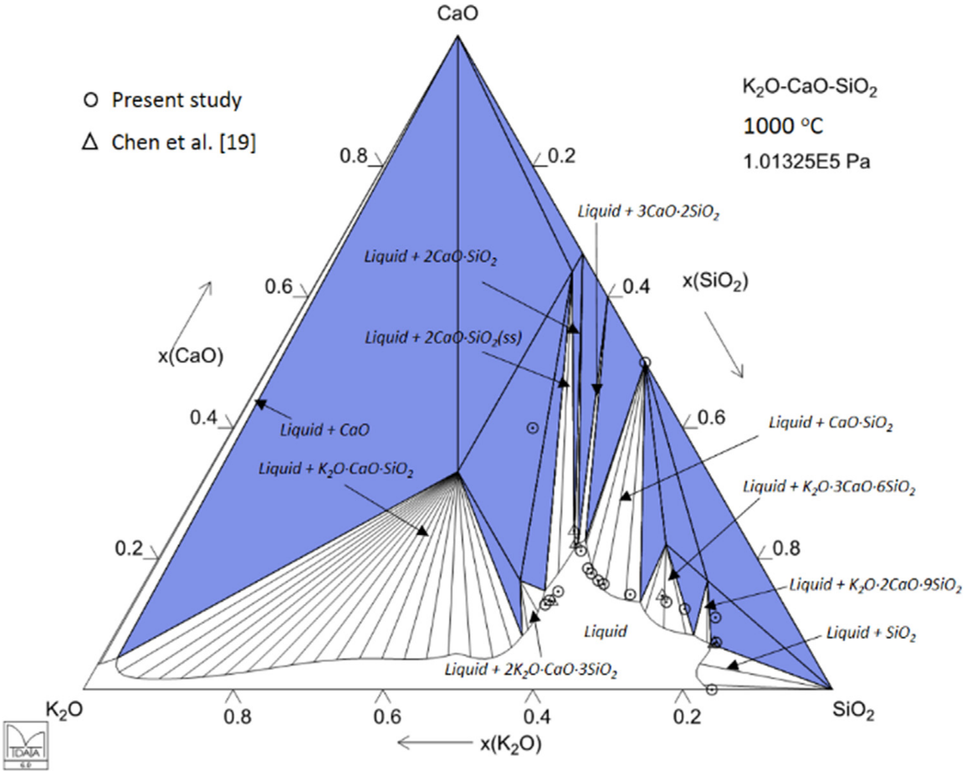

Fig. 8. Isothermal section at 1000 °C calculated by MTDATA [20] using Mtox vers. 8.2 database [21].

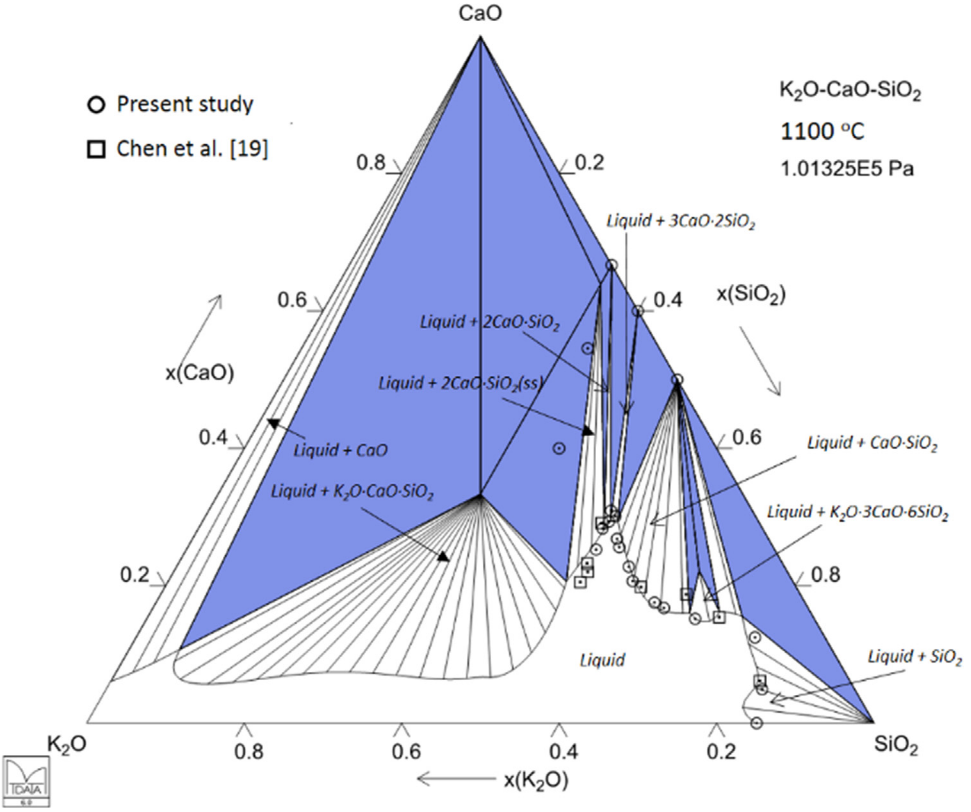

Fig. 9. Isothermal section at 1100 °C calculated by MTDATA [20] using Mtox vers. 8.2 database [21].

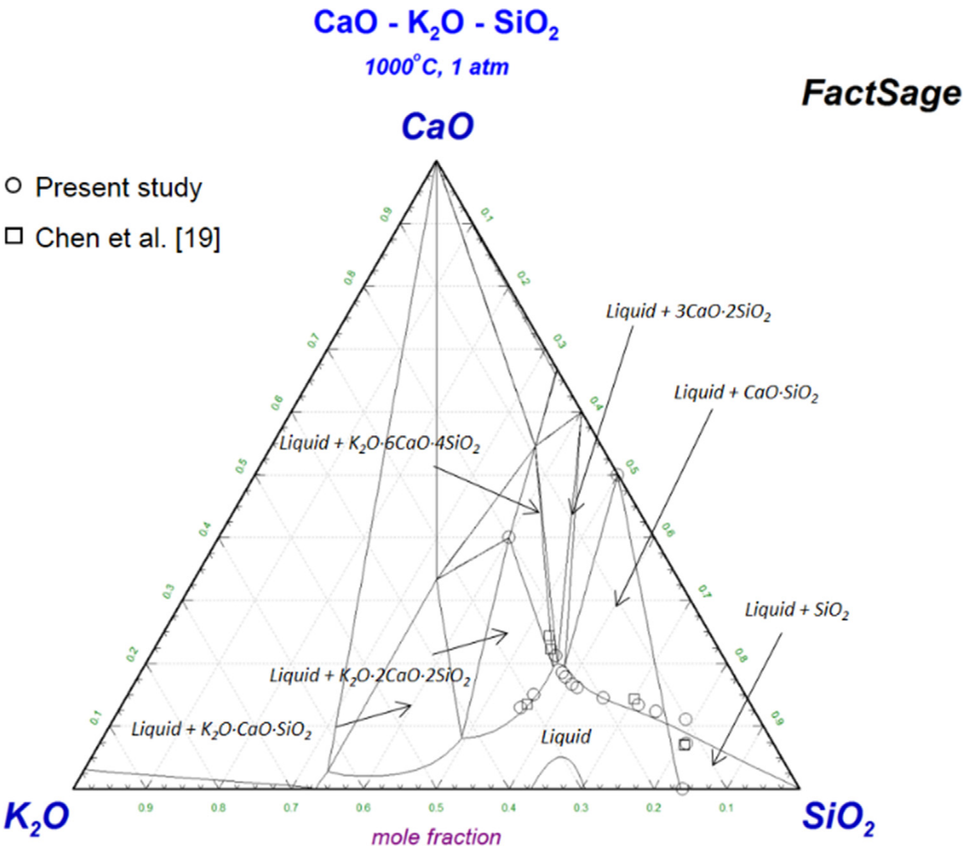

Fig. 10. Isothermal section at 1000 °C calculated by FactSage [22].

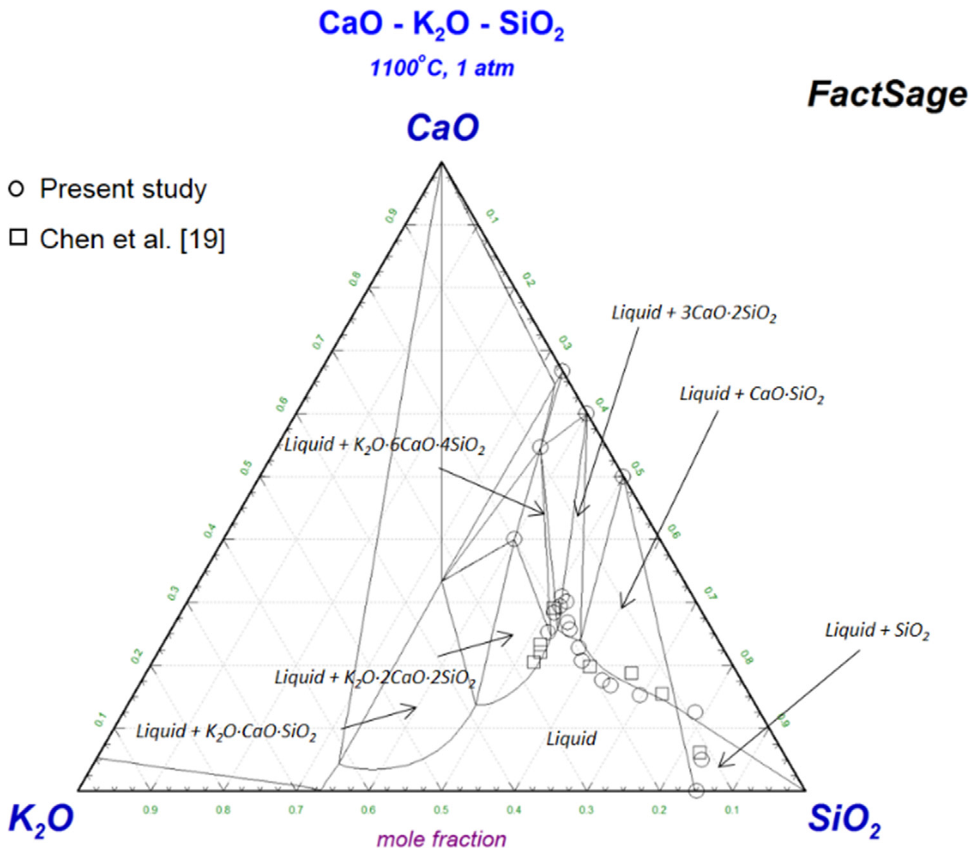

Fig. 11. Isothermal section at 1100 °C calculated by FactSage [22].

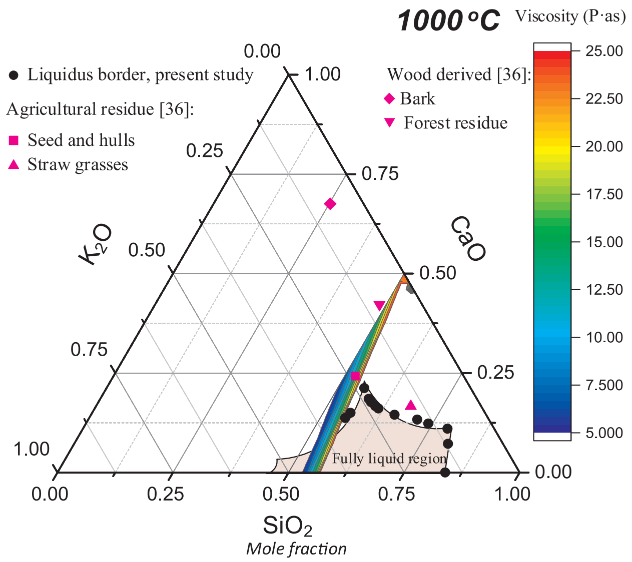

Fig. 12. Viscosity and liquidus boundary obtained in the present investigation at 1000 °C.

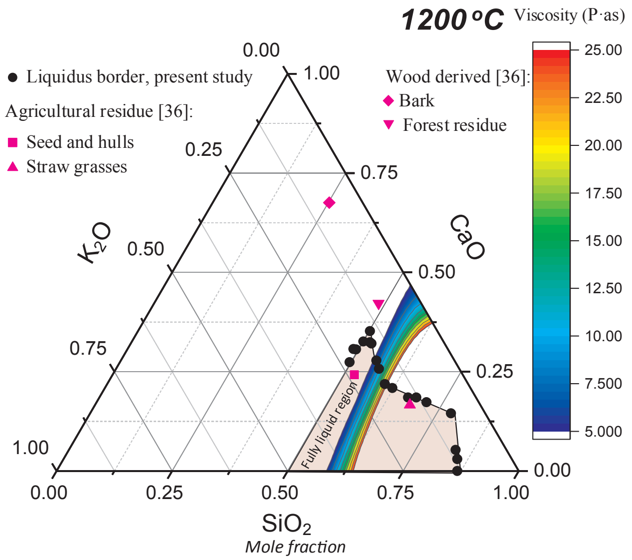

Fig. 13. Viscosity and liquidus boundary obtained in the present investigation at 1200 °C.

calculated line lies under the experimental data generated from the present investigation, as indicated in Fig. 11. In the present study, the liquid at double saturation with $K_2O{\cdot}6CaO{\cdot}4SiO_2$ and $2CaO{\cdot}SiO_2$, indicating the location of intersection between these two primary fields, was obtained at 1100 °C (Fig. 4J).

3.8. Primary phase field of $K_2O{\cdot}2CaO{\cdot}2SiO_2$

In the present study, the liquidus line in equilibrium with $K_2O{\cdot}2CaO{\cdot}2SiO_2$ was in a good agreement with the experimental data by Chen et al. [19] and the calculated contour by FactSage [22]. However, MTDATA [20,21] calculation indicate that the liquidus boundaries are in equilibrium with $2K_2O{\cdot}CaO{\cdot}3SiO_2$ and $2CaO{\cdot}SiO_2$ solid solutions at 1000 and 1100 °C, respectively as can be seen in Figs. 8 and 9, respectively.

Based on the present investigation, it can be seen in Fig. 6B that $CaO{\cdot}SiO_2$, $3CaO{\cdot}2SiO_2$, $2CaO{\cdot}SiO_2$, $K_2O{\cdot}6CaO{\cdot}4SiO_2$ and $K_2O{\cdot}2CaO{\cdot}2SiO_2$ compounds can still be in equilibrium with a liquid at

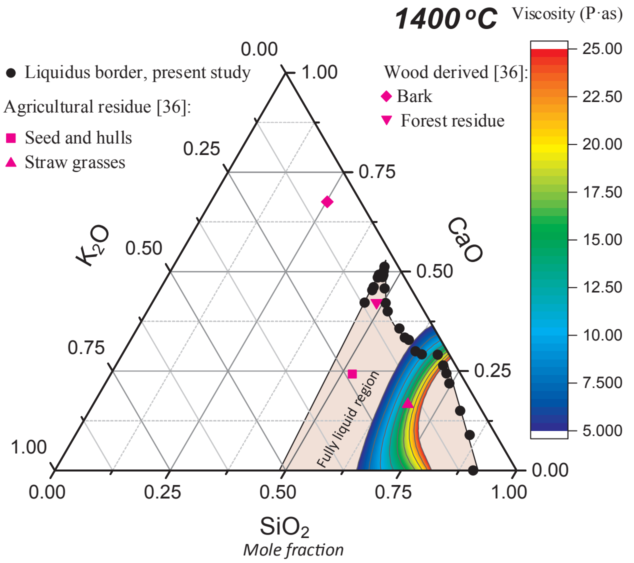

Fig. 14. Viscosity and liquidus boundary obtained in the present investigation at 1400 °C.

1100 °C. However, at 1000 °C the $CaO{\cdot}SiO_2$ primary phase field intersects $K_2O{\cdot}2CaO{\cdot}2SiO_2$ as indicated in Fig. 6A. It means that between 1100 and 1000 °C there are peritectic points at which the primary phase fields of $3CaO{\cdot}2SiO_2$, $2CaO{\cdot}SiO_2$ and $K_2O{\cdot}6CaO{\cdot}4SiO_2$ disappeared upon cooling. Therefore, if temperature is cooled from 1100 °C to 1000 °C, present study suggests a sequence of peritectic reactions that happen. First primary phase field that disappeared is $2CaO{\cdot}SiO_2$ through reaction of $L + 2CaO{\cdot}SiO_2 \leftrightarrow 3CaO{\cdot}2SiO_2 + K_2O{\cdot}6CaO{\cdot}4SiO_2$ (1). Then, it is followed by the removal of $3CaO{\cdot}2SiO_2$ primary phase field with the reaction of $L + 3CaO{\cdot}2SiO_2 \leftrightarrow K_2O{\cdot}6CaO{\cdot}4SiO_2 + CaO{\cdot}SiO_2$ (2). After that, $K_2O{\cdot}6CaO{\cdot}4SiO_2$ primary phase field vanished with the reaction of $L + K_2O{\cdot}6CaO{\cdot}4SiO_2 \leftrightarrow K_2O{\cdot}2CaO{\cdot}2SiO_2 + CaO{\cdot}SiO_2$ (4). Therefore, at 1000 °C the primary phase field of $K_2O{\cdot}2CaO{\cdot}2SiO_2$ intersects the primary phase field of $CaO{\cdot}SiO_2$. This sequence was also reported by Kim [23] although the calculation of these three peritectic reactions did not occur between 1100 and 1000 °C. Therefore, the data obtained in the present equilibrium study can be utilized for reassessing the K_2O-CaO-SiO_2 system.

3.9. *Viscosity of liquid phase*

Entrained flow gasification of biomass is a promising technology for production of syngas and subsequently liquid biofuels in various biorefinery concepts [9]. For fuels with high ash contents, a slagging wall concept is used, where a layer of slag is formed on the walls, with a completely molten layer towards the flame side and a solidified slag/ash towards the refractory wall of the reactor. Typically, temperatures in the reactor are above 1200 °C. One important factor for the operation of the reactor is the viscosity of the molten slag. The optimal range of the viscosity is typically 8–25 Pa·s [9,33]. Kondratiev and Jak [34] reported the optimal range of 5–25 Pa·s for coal slags. If the slag viscosity is too high and the slag flow is too slow, it may lead to build-up of slag and blocking of the tap hole of the reactor, which can lead to unscheduled shutdowns. If the viscosity is too low, the slag layer may be discontinuous or the increased flow velocity may increase the wear of refractories.

Therefore, for optimal operations of such as slagging gasifier, the following criteria should be fulfilled, among other criteria: The composition of the ash-forming elements in the fuel should be such that the slag is close to be fully molten and that the viscosity of the molten phase falls between 8 and 25 Pa·s at the operating temperatures. For the simplified K_2O-CaO-SiO_2 system, the temperature-composition domain for fully liquid slags has now been determined experimentally and compared with thermodynamic modelling in the present study.

In a recent paper by Chen and Zhao [35], the viscosity of six different compositions in the K_2O-CaO-SiO_2 system were measured at temperatures between 1000 and 1600 °C. They also compared the measured results with different viscosity models and showed that the viscosity model available in the Factsage [36] gives the best predictions compared to their experimental data.

In the present study, by using the viscosity model available in the Factsage 7.3 [22], the viscosity of the fully molten slag was calculated at 1000, 1200 and 1400 °C and superimposed with the liquid phase region at these temperatures to identify compositional ranges where the slag is completely molten and has a viscosity between 5 and 25 Pa·s. In addition, compositions of the ash forming elements from different biomass types were taken from the Åbo Akademi chemical fractionation database [37], to assess which biomass types are suitable for specific temperature-composition ranges.

It can be seen in Fig. 12 that at 1000 °C, fuels or fuels/additives mixtures containing high potassium and low calcium are needed to attain the conditions for a fully liquid slag and suitable viscosity. At 1200 °C (Fig. 13), blends of agricultural residues (seed and hulls and straw grasses) have a suitable composition to attain optimal viscosity because the blended composition can be located in fully liquid area and the optimum viscosity value between 5 and 25 Pa·s. Whereas for wood derived-fuels, higher temperature and SiO_2 fluxing are needed to bring the final composition of the mixtures to the optimum region, as shown for 1400 °C (Fig. 14).

To attain optimal conditions at the temperatures of interest, one option may be to use additives to optimize the composition and viscosity of the liquid. Potential additives could be silica sand, lime and K_2CO_3. Silica sand would probably be the most practically and economically feasible option, but the addition of a potassium source may be needed if lower gasification temperatures are used. However, higher fraction of potassium may also lead to increased vaporization, which in turn can cause corrosion and degradation of the gasifier material.

4. Conclusion

In the present study, liquidus compositions in the primary phase fields of SiO_2, $CaO{\cdot}SiO_2$, $3CaO{\cdot}2SiO_2$, $2CaO{\cdot}SiO_2$, $K_2O{\cdot}6CaO{\cdot}4SiO_2$ and $K_2O{\cdot}2CaO{\cdot}2SiO_2$ have been investigated between 1000 and 1400 °C, by using an equilibration-quenching-EPMA/EDS analysis method. The liquidus projections and isothermal sections of the $K_2O{\cdot}CaO{\cdot}SiO_2$ system at two and three phase saturations have been generated. Liquidus compositions at several primary phase fields obtained in the present study indicated a good agreement with previous experimental measurements by Morey et al. [1] and Chen et al. [19] and also with calculated phase diagrams by MTDATA [20,21] and FactSage [23,23] at certain temperatures. Some novel data also have been obtained to support the previous predictions which include the liquidus data at $3CaO{\cdot}2SiO_2$ saturation and at double saturation of $3CaO{\cdot}2SiO_2$ and $CaO{\cdot}SiO_2$ and also $CaO{\cdot}SiO_2$ and SiO_2 that has been never published.

Combining the phase equilibrium data with calculated viscosity of K_2O-CaO-SiO_2 slags, it can be used for proposing slag compositions preferable to be used in entrained flow biomass gasifiers with minimal operational challenges related to the ash and slag flow, thus maximizing the efficiency and availability of the gasifier.

Declaration of Competing Interests

The authors declare that they have no known competing financial interests or personal relationships that could have appeared to influence the work reported in this paper

Acknowledgements

The research was financially supported by the FLASH project (Predicting the flow behavior of ash mixtures for production of transport biofuels in the circular economy, project number 280892) within the EnergiX program by the Norwegian Research Council, Norway. Academy of Finland's RawMatTERS Finland Infrastructure (RAMI) based at Aalto University, VTT Technical Research Centre and Geological Survey of Finland (GTK), were employed in this investigation. EPMA analysis done by Mr. Lassi Pakkanen GTK is also greatly acknowledged.

References

[1] Morey GW, Kracek FC, Bowen NL. The ternary system K_2O-CaO-SiO_2. J Glass Technol 1930;14:149–87.

[2] Morey GW, Kracek FCFC, Bowen NL. The ternary system K_2O-CaO-SiO_2: a correction. J Soc Glass Technol 1931;15:57.

[3] Levin EM, McMurdie HF, Robbins CR. Phase diagrams for ceramists. Am Ceram Soc 1964.

[4] Verein Deutscher Eisenhüttenleute. Slag atlas. Düsseldorf: Verlag Stahleisen GmbH; 1995.

[5] Tripathi H, Hira SK, Kumar AS, Gupta U, Manna PP, Singh SP. Structural characterization and in vitro bioactivity assessment of SiO_2–CaO–P_2O_5–K_2O–Al_2O_3 glass as bioactive ceramic material. Ceram Int 2015;41(9):11756–69.

[6] Kim WH, Sohn I, Min DJ. A study on the viscous behavior with K_2O additions in the CaO-SiO_2-Al_2O_3-MgO-K_2O quinary slag system. Steel Res Int 2010;81(9):735–41.

[7] Li Y, Wu J, Ma W, Yang B. Boron removal from metallurgical grade silicon using a refining technique of calcium silicate molten slag containing potassium carbonate. Silicon 2015;7(3):247–52.

[8] Vassilev SV, Baxter D, Andersen LK, Vassileva CG. An overview of the composition and application of biomass ash. Part 1. Phase–mineral and chemical composition and classification. Fuel 2013;105:40–76.

[9] Carlsson P, Ma C, Molinder R, Weiland F, Wiinikka H, Öhman M, et al. Slag formation during oxygen-blown entrained-flow gasification of stem wood. Energy Fuels 2014;28(11):6941–52.

[10] Seebold S, Eberhard M, Wu G, Yazhenskikh E, Sergeev D, Kolb T, et al. Thermophysical and chemical properties of bioliq slags. Fuel 2017;1(197):596–604.

[11] Ma C, Backman R, Öhman M. Thermochemical equilibrium study of slag formation during pressurized entrained-flow gasification of woody biomass. Energy Fuels 2015;29(7):4399–406.

[12] He H, Ji X, Boström D, Backman R, Öhman M. Mechanism of quartz bed particle layer formation in fluidized bed combustion of wood-derived fuels. Energy Fuels 2016;30(3):2227–32.

[13] Yao Y, Hamada E, Sato K, Akiyama T, Yoneyama T. Identification of the major constituents of fused potassium silicate fertilizer. ISIJ Int 2014;54(4):990–3.

[14] Ohsato H, Sugimura T, Hayashi S, Ogihara T. β-Wollastonite and para-wollastonite precipitated from the join K_2O-$CaSiO_3$. Bull Nagoya Inst Technol 1980;32:123–30.

[15] Risnes H. High temperature filtration in biomass combustion and gasification processes [PhD. thesis]. Norwegian University of Science and Technology, Department of Thermal Energy and Hydropower; 2002.

[16] Taylor WC. The system $2CaO{\cdot}SiO_2$-$K_2O{\cdot}CaO{\cdot}SiO_2$ and other phase-equilibrium studies involving potash. Portland Cement Association Fellowship at the National Bureau of Standards; 1941.

[17] Arroyabe E, Tessadri R, Többens DM, Kahlenberg V. Does K_2CaSiO_4 exist? A phase-analytical study in the system K_2O–CaO–SiO_2 with implications for the characterization of residual materials. J Am Ceram Soc 2011;94(8):2652–5.

[18] Bankole LK, Hamid A, Sheikh SR, Nurulakmal MS. Crystallization of potassium calcium silicate from modified industrial EAF slag. Adv Mat Res. 2013;620:66–71.

[19] Chen M, Hou X, Chen J, Zhao B. Phase equilibria studies in the SiO_2-K_2O-CaO system. Metall Mater Trans B 2016;47(3):1690–6.

[20] Davies RH, Dinsdale AT, Gisby JA, Robinson JA, Martin AM. MTDATA-thermodynamic and phase equilibrium software from the National Physical Laboratory. Calphad 2002;26(2):229–71.

[21] Gisby J, Taskinen P, Pihlasalo J, Li Z, Tyrer M, Pearce J, et al. MTDATA and the prediction of phase equilibria in oxide systems: 30 years of industrial collaboration. Metall Mater Trans B 2017;48(1):91–8.

[22] Bale CW, Bélisle E, Chartrand P, Decterov SA, Eriksson G, Hack K, et al. FactSage thermochemical software and databases—recent developments. Calphad 2009;33(2):295–311.

[23] Kim DG. Coupled experimental study and thermodynamic optimization of the K_2O-Na_2O-CaO-MgO-Al_2O_3-SiO_2 system [PhD. thesis]. McGill University, Department of Mining and Materials Engineering; 2017.

[24] Zhang L, Schmetterer C, Masset PJ. Thermodynamic Modelling of the CaO-SiO_2-M_2O (M= K, Na) Systems. High Temp Mat Pr-Isr 2013;32(3):223–8.

[25] Arroyabe E, Prechtel F, Többens DM, Kaindl R, Kahlenberg V. $K_2Ca_3Si_3O_{10}$, a novel trisilicate: high-pressure synthesis, structural, spectroscopic and computational studies. Eur J Mineral 2011;23(3):425–35.

[26] Schmidmair D, Kahlenberg V, Perfler L, Tribus M, Hildebrandt J, Többens DM. On the ambient pressure polymorph of $K_2Ca_3Si_3O_{10}$—an unusual mixed-anion silicate and its structural and spectroscopic characterization. J Solid State Chem 2015;228:90–8.

[27] Schmidmair D, Kahlenberg V, Grießer A. $K_2CaSi_4O_{10}$: a novel phase in the ternary system K_2O–CaO–SiO_2 and member of the litidionite group of crystal structures. Am Ceram Soc 2018;101(2):919–27.

[28] Santoso I, Taskinen P. Phase equilibria study in the TeO_2-Na_2O-SiO_2 system in air between 723 K (500 °C) and 1473 K (1200 °C). Metall Mater Trans B 2016;47(4):2440–6.

[29] Akdogan G, Johto H, Taskinen P. Phase equilibria study of K-O–Si system in equilibrium with air. J Eur Ceram Soc 2014;34(15):4053–8.

[30] Grundy AN, Liu H, Jung IH, Decterov SA, Pelton AD. A model to calculate the viscosity of silicate melts: part I: viscosity of binary SiO2# x2013; MeO x systems (Me= Na, K, Ca, Mg, Al). Int J Mater Res 2008;99(11):1185–94.

[31] Suzukawa Y. The alkali phases in portland cement: III, Influence of Na_2O on the mineral composition of portland cement. Zem Kalk-Gips 1956;9:433–6.

[32] Fedorov NF, Brodkina ER. Solid solutions in the system $2CaO{\cdot}SiO_2$-$K_2O{\cdot}CaO{\cdot}SiO_2$. Izv An Sssr Neorg Mater 1967;3:1283–4.

[33] Ma C, Carlborg M, Hedman H, Wennebro J, Weiland F, Wiinikka H, et al. Ash formation in pilot-scale pressurized entrained-flow gasification of bark and a bark/peat mixture. Energy Fuels 2016;30(12):10543–54.

[34] Kondratiev A, Jak E. Predicting coal ash slag flow characteristics (viscosity model for the Al_2O_3–CaO–'FeO'–SiO_2 system). Fuel 2001;80(14):1989–2000.

[35] Chen M, Zhao B. Viscosity measurements of the SiO_2–K_2O–CaO system relevant to biomass slags. Fuel 2016;180:638–44.

[36] Kim WY, Pelton AD, Decterov SA. A model to calculate the viscosity of silicate melts: Part III: Modification for melts containing alkali oxides. Int J Mater Res 2012;103(3):313–28.

[37] Laboratory of Inorganic Chemistry at ÅA University. Åbo Akademi Chemical Fractionation Database; 2012 [cited 23 August 2019]. Available from https://web.abo.fi/fak/tkf/ook/bransle/.